JOURNAL OF CATALYSIS 48, 374–385 (1977)

Sorption and Temperature-Programmed Desorption of Hydrogen from Palladium and from Palladium on Activated Carbon

J. A. KONVALINKA AND J. J. F. SCHOLTEN[1]

Central Laboratory, DSM, P.O. Box 18, Geleen, The Netherlands

Received September 9, 1976; revised March 18, 1977

The chemisorption of hydrogen on palladium has been studied by measuring pulse-wise adsorption and temperature-programmed desorption (TPD) on various palladium samples and on palladium-on-activated-carbon catalysts. The desorption of weakly bound ("type C") hydrogen is found to be first order in coverage, and the enthalpy of adsorption is about 34 kJ/mole. Its population is proportional to the amount of weakly adsorbed hydrogen ("type C" hydrogen), and a desorption mechanism is postulated in which a subsurface hydrogen recombines with a surface hydrogen atom ("breakthrough" mechanism). The desorption of strongly bound hydrogen is second order in coverage, and the enthalpy of adsorption on Pd on activated carbon is 90 ± 5 kJ/mole, a value about equal to that found by E. Conrad, G. Ertl, and E. E. Latta [*Surface Sci.* 41, 435 (1974)], for palladium(111). Its population is equal to the amount of hydrogen pulsed, minus half the amount of "type C" hydrogen desorbed, in accordance with the proposed "breakthrough" mechanism. Large amounts of electropositive contaminations in palladium, like Zn, Pb, and Ca, suppress "type C" adsorption, whereas the enthalpy of adsorption of strongly bound hydrogen decreases to lower values.

INTRODUCTION

Because a striking analogy exists between hydrogen chemisorption on nickel and on palladium, we will first mention the most relevant data for the nickel. Sweet and Rideal (*1*), measuring isosteres on polycrystalline nickel, detected weakly adsorbed hydrogen (ΔH is 25–43 kJ/mole), besides an equal amount of less mobile strongly bound hydrogen (ΔH is 83–100 kJ/mole). Christmann *et al.* (*2*) and Lapujoulade and Neil (*3*), in LEED studies of hydrogen on Ni(111), (110), and (100), found only the strongly held form, the enthalpy of adsorption being about 96 kJ/mole at low coverage on all three planes.

Weakly bound hydrogen is not perceptible in the LEED studies, presumably due to the relatively low pressures applied. The occurrence of a weak type of hydrogen adsorption on nickel (often called "type C" hydrogen in the literature) was, however, confirmed in a TPD study by Bendorf and Thieme (*4*). In connection with the Pd results reported in this article, it is interesting to note that the weakly adsorbed hydrogen on nickel presented a desorption behavior first order in coverage.

Less is known about hydrogen chemisorption on palladium. A flash-filament study by Aldag and Schmidt (*5*) showed four desorption peaks, corresponding to enthalpies of adsorption of 58, 92, 104.6, and 146.4 kJ/mole. Single-crystal results by Conrad and co-workers (*6*) for Pd(111)

---

[1] To whom all correspondence should be addressed.

ISSN 0021-9517

and Pd(110) confirm these findings, except for the weak and very strong chemisorption; on Pd(111), an enthalpy of adsorption of 88 kJ/mole is arrived at, and, on Pd(110), a value of 102 kJ/mole is found.

Enthalpies and entropies of weak hydrogen chemisorption on palladium wire and black are reported by Lynch and Flanagan (*7*). One important conclusion of their work is that weak "type C" chemisorption is an adsorption in excess of the strongly held monolayer. It is suggested by these authors that it is located in surface interstitial sites and, thus, is a natural precursor to interstitial *ab*sorbed hydrogen. The isosteric enthalpy of adsorption varies from 44.8 (at an excess coverage of 0.06) to 36.4 kJ/mole (at an excess coverage of 0.3) and, hence, is of the same magnitude as the values found by the other workers for palladium and for nickel as well.

The nature of the weak chemisorption is in doubt; some workers have suggested that it is molecular (*8*, *9*), and others that it is atomic (*10*).

It is the aim of the present article to show that TPD spectra of hydrogen desorbing from palladium on activated carbon lead to results in reasonable accordance with the UHV results of Conrad *et al.* (*6*) for Pd(111) single-crystal planes, as far as strong bonding is considered. Our results for weak "type C" adsorption are quantitatively in accordance with the results of Lynch and Flanagan (*7*) mentioned above. The location of this hydrogen in interstitial surface sites was not adopted by us. A new type of hydrogen bonding is suggested, which is in accordance with all experimental evidence now available. Finally, the influence of electropositive contaminations on the binding strength of hydrogen on palladium is briefly discussed.

EXPERIMENTAL

a. Apparatus

A stainless steel grease- and mercury-free apparatus was constructed in which hydrogen could be adsorbed pulse-wise on the samples, and in which TPD spectra could be measured under conditions in which readsorption could occur freely (Fig. 1).

Theoretical analysis of the TPD spectra is performed according to Cvetanović and Amenomiya (*11*) and Konvalinka *et al.* (*12*).

The carrier gas argon (99.998% purity) was further purified via a cartridge filled with a highly reduced 50% Ni-on-silica Harshaw catalyst and an equal amount of Type 3A molecular sieves, $\frac{1}{16}$-in. pellets,

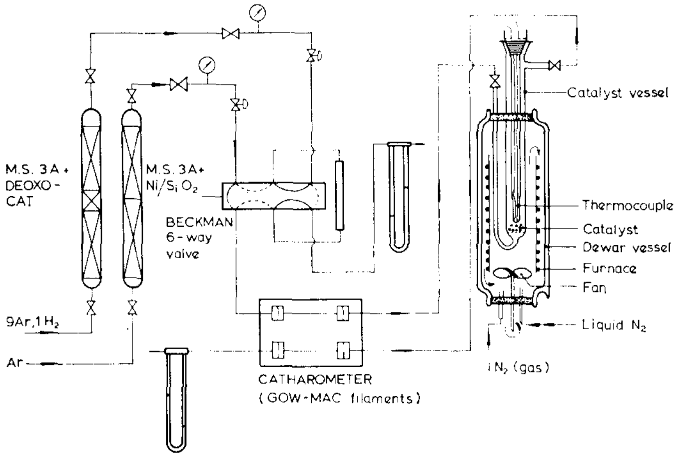

FIG. 1. Scheme of the TPD apparatus.

from Union Carbide, activated in hydrogen at 400°C. The pulse gas was a mixture of 10% hydrogen (N_2: 100 ppm; O_2: 5 ppm; CO: 5 ppm; H_2O: 100 ppm) and 90% argon carrier gas. It was further purified via a layer of Type 3A molecular sieve, a layer of Deoxo catalyst D (0.5% Pd on γ-alumina, from Engelhard, U.S.A.), and a second layer of Type 3A molecular sieve.

Automatic pulsing of the argon–hydrogen mixture in the carrier gas stream was performed by means of a Beckman six-way chromatography valve with a pulse volume of 0.78 cm^3.

The furnace construction is indicated in Fig. 1. Linear time–temperature schedules in the range of 133–775°K were electronically regulated via the signal of a Pt 100-ohm resistance; heating rates between 1 and 30°K/min could be realized. Above 310°K, the electrical furnace was used; below that temperature, heating with the furnace was combined with cooling by means of a haze of liquid nitrogen, which was injected in a circulating stream of nitrogen gas in the furnace.

Hydrogen concentrations in the carrier gas were measured catharometrically and were recorded automatically.

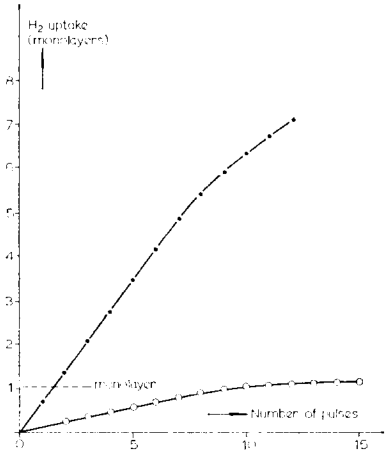

FIG. 2. Pulse-wise hydrogen chemisorption at 233°K. Open circles: Pd black, sample 2, contaminated. Filled circles: Pd sponge, sample 4, high purity.

b. *Samples: Their Texture and Analysis*

Sample 1: 9.4 wt% Pd on activated carbon. Sample 1 was prepared according to Dutch Patent Application 7502968; filing date: March 13, 1975. H_2PdCl_4, from Degussa, Germany, purity 99.8%, is adsorbed from an aqueous solution on the activated carbon, followed by basic hydrolysis and reduction by adding a mixture of an aqueous $NaHCO_3$ solution in methanol and drying at 120°C. The activated carbon was from Degussa, Germany, Type Carbopuron 4N, ash free; analysis: Ca < 0.04 wt%, Fe < 0.03 wt%, Cu < 0.005 wt%, and Pb < 0.001 wt%; BET surface area: 895 m^2/g. Auger surface analysis showed S to be the only surface impurity, its concentration being less than 0.01 monolayer.

From electron microscopy, the diameters of the Pd crystallites were found to be between 2 and 11 nm, whereas, from CO chemisorption (*13*), a mean volume–surface diameter of 6.4 nm was found.

Sample 2: palladium black. Sample 2, from Drijfhout, Amsterdam, had a BET surface area of 6 m^2/g. ESCA analysis showed Pb and Zn to be the main surface impurities; the Zn surface concentration was of the order of 5–10 atom% and the Pb surface concentration was 3 atom% maximum.

Sample 3: palladium Mohr. Sample 3 from Degussa, Germany, had a BET surface area of 18 m^2/g, but the free-metal surface area, determined from CO chemisorption (*13*), was found to be only 10 m^2/g, which indicates a high degree of contamination. ESCA analysis showed carbon to be a possible surface impurity, but there is uncertainty about its concentration due to carbon signals from the fixation tape. Sodium was just detectable as a surface impurity. Ca might be present, but its emission line is very near that of Pd, which makes a more quantitative determination impossible.

Sample 4: spec.pure palladium sponge: Sample 4 was purchased from Johnson Matthey & Co., Ltd., England, and was reduced in ultrapure hydrogen. The BET surface area, calculated from the methane adsorption isotherm at −196°C, was 0.34 m²/g. ESCA analysis showed its surface to be very pure; only very small amounts of sodium and chlorine could be detected, which may have resulted from the glass envelope in which the sample was packed before surface analysis.

c. *Pretreatment of the Samples*

Before pulse loading and measuring TPD spectra, all samples were heated *in situ* in a stream of argon, purified as indicated before, at 170°C, after which argon was replaced by hydrogen purified via a palladium thimble. Then, the temperature was slowly raised to 300°C, and reduction was carried out for 3 hr. To remove all hydrogen from the sample, hydrogen was replaced by argon; the temperature was raised to 500°C and, after 2–3 hr, was brought to 400°C. Heating in argon at 400°C was stopped when the gas was virtually free of hydrogen.

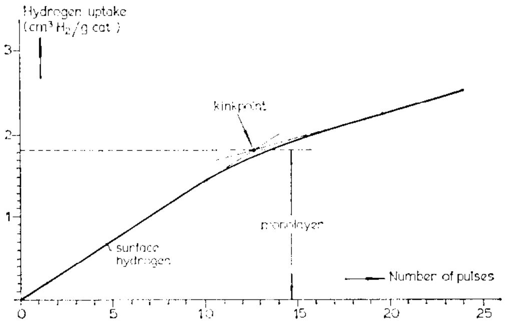

FIG. 3. Pulse-wise hydrogen chemisorption at 233°K, sample 1, Experiment 1, Table 1.

RESULTS

a. *Pulse Experiments*

Pulse-wise adsorption of hydrogen on samples 2 and 4 at 233°K is represented in Fig. 2. The maximum partial pressure during pulse adsorption was 300 N m^{-2}; under this condition, only the α phase of bulk palladium hydride could be formed. Sample 2 showed a hydrogen uptake of only one monolayer; obviously, the high concentration of surface impurities prevented penetration of hydrogen into the bulk.

The very pure palladium sponge, sample 4, rapidly took up all hydrogen pulses;

TABLE 1

Sample 1: Amounts of Adsorbed and Desorbed Hydrogen in a Continuous Series of Pulse and TPD Experiments

Expt No. (1)[a]	V_{des}/V_{ads} (2)	Total H_2 pulsed [cm³(NTP)/g of cat] (3)	Pulsed up to the kinkpoint [cm³(NTP)/g of cat] (4)	S_{rel} (5)	Hydrogen in excess of a monolayer [cm³(NTP)/g of cat] Desorbed (6)	Hydrogen in excess of a monolayer [cm³(NTP)/g of cat] Not desorbed (7)
1	0.93	2.63	1.84	0.97	0.65	0.18
2	1.06	0.49		1.0[b]	0.00	0.00
3	1.05	0.98		1.0[b]	0.00	0.00
4	0.74	3.23	1.90	1.0	0.49	0.84
5	0.85	2.05	1.55	0.82	0.19	0.31
6	0.73	2.80	1.33	0.70	0.72	0.76
7	0.74	2.45	1.30	0.68	0.51	0.64

[a] Column number.

[b] These relative surface areas were not determined. The value 1.0 is based on the fact that, in Expt 4, S_{rel} is 1.0, and, hence, between Expt 1 and 4, no sintering occurred.

besides formation of the monolayer, bulk α-palladium hydride was rapidly formed.

Hence, one might think that the ab/adsorption behavior gives a useful indication of the degree of surface purity. This, however, is not always the case. Via a special technique (*14*), germanium was incorporated in the surface of the palladium crystallites in sample 1, up to a Ge coverage of 0.85 Ge atoms per surface palladium atom still accessible for hydrogen chemisorption. Details will be given in future papers. This sample rapidly took up both surface and subsurface hydrogen.

Hydrogen adsorption, as a function of the number of pulses on sample 1, is plotted in Fig. 3. From the first 10 to 11 pulses, hydrogen was rapidly and totally taken up by the sample, but, beyond the kinkpoint indicated in Fig. 3, only part of the hydrogen was taken up.

The sorption behavior depicted in Fig. 3 appeared to be reproducible, and it was observed in at least 50 experiments with Pd-on-carbon and Pd/Ge-on-carbon samples.

The amount of hydrogen chemisorbed in a monolayer was calculated by the extrapolation method indicated in Fig. 3. In order to determine the reliability of this method, a CO chemisorption experiment was performed with a parallel sample from the same batch which underwent exactly the same pretreatment procedure as did sample 1. From CO chemisorption (*13*), a free-palladium surface area of 7.5 m^2 Pd/g of catalyst was arrived at, whereas, from Fig. 3, a value 6.78 m^2 Pd/g of catalyst is found. In the calculation of the free-palladium surface area from hydrogen chemisorption up to the kinkpoint, it was assumed that, according to Sundquist (*15*), 70% (111), 25% (100), and 5% (110) planes are exposed by the Pd crystallites, from which a mean surface concentration of 1.45×10^{19} Pd sites/m^2 is calculated. Furthermore, Aben's (*16*) surface stoichiometry of one hydrogen per surface palladium atom was accepted.

Sermon (*17*) arrived at a good correspondence between the surface area data measured by BET and those measured by hydrogen chemisorption techniques, assuming a H/Pd surface stoichiometry of unity and an average number of surface palladium atoms of $1.2 \times 10^{19}/m^2$. On this basis, our kinkpoint method resulted in a free-Pd surface area of 8.19 m^2 Pd/g of catalyst.

With sample 1, a continuous series of successive pulse and TPD experiments was carried out. Between each experiment, the sample was heated in a stream of very pure argon at 773°K for 2 or 3 hr in order to desorb any hydrogen possibly remaining from the previous experiment. The second column in Table 1 presents the ratio of totally desorbed hydrogen, calculated from the integrated TPD peak areas, to totally adsorbed hydrogen, calculated from the previous pulse experiment. In experiments 2 and 3, in which less than one monolayer was pulsed, this ratio is about 1. In experiments 1 and 4–7, in which, in addition to the formation of the chemisorbed layer, more hydrogen was taken up, part of this hydrogen in excess did not desorb during the succeeding 1-hr TPD run between 232 and 773°K, followed by the argon treatment indicated above. This is the reason that V_{des}/V_{ads} in these experiments is less than unity.

Incomplete desorption of hydrogen from palladium crystallites with diameters between 2 and 11 nm is difficult to conceive, as the rate of interstitial diffusion of hydrogen in palladium is extremely high compared with other metals, the activation energy of diffusion being only 23.4–25.1 kJ/g-atom (*18*). Therefore, the most probable explanation for the fact that part of the hydrogen pulsed in excess of a monolayer does not desorb, is the occurrence of hydrogen spillover from the small palladium crystallites to the surface of the activated carbon carrier, by analogy with the findings of

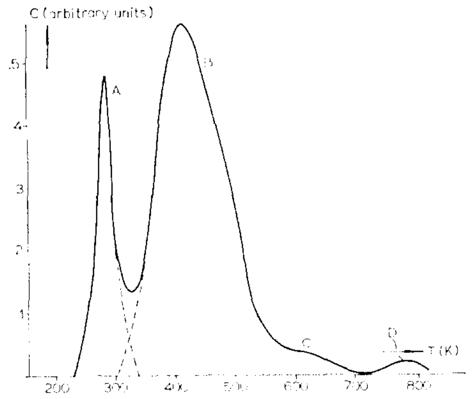

FIG. 4. TPD spectrum for hydrogen on palladium, sample 1, experiment 1. Heating rate $\beta = 10°K/min$. Peak maxima at 293, 407, 643, and 780°K.

Boudart and Aldag (*19*) for the case of hydrogen adsorption on platinized carbon. It is likely that the spilled-over hydrogen reacts with the various oxygen-containing surface groups on the surface of the activated carbon (*20*).

Column 3 in Table 1 indicates the total amount of pulsed hydrogen, and columns 4 and 5, respectively, give the amount of hydrogen pulsed up to the kinkpoint (see Fig. 3) and the relative free-palladium surface area calculated from it. It is seen that, in the course of the experiments, the free-palladium surface area gradually decreases, obviously due to sintering at the relatively high TPD top temperature of 773°K and the high temperature during the intermediate sample pretreatment between experiments (2–3 hr at 773°K in argon). Finally, column 6 gives the amount of desorbed hydrogen in excess of the amount pulsed up to the kinkpoint, and column 7, the volume of hydrogen which did not desorb.

b. Comparison of Pulse and TPD Results

As an example, Fig. 4 gives the TPD spectrum of hydrogen desorbing from sample 1, after pulse loading up to a coverage 1.46. Two major peaks are observed with maxima at $T_M = 293$ and 407°K. Furthermore, low-area peaks are found with maxima at 640 and 780°K. The integrated peak surface area of these last peaks is less than 2% of the area of the second major peak. In all cases in which more than one monolayer of hydrogen was pulsed, this type of TPD spectrum was obtained.

Two important observations were made: (i) Starting at coverage <1, peak A was always absent. (ii) Peak A could only be described as a desorption first order in coverage, as will be shown in the next section. Statement (i) is related to the experiments 2 and 3 in Table 1, in which coverages of 0.27 and 0.55, respectively, were calculated. An additional experiment was performed with the same catalyst, pulse loaded up to a coverage 0.96, and, indeed, only peak B was observed in the subsequent TPD run. This sample, however, was preloaded with 5 atom% Ge [see Ref. (*14*)].

a) Porthole mechanism I

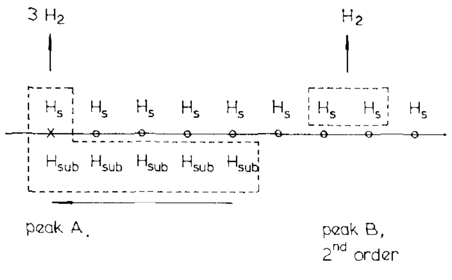

b) Breakthrough mechanism II

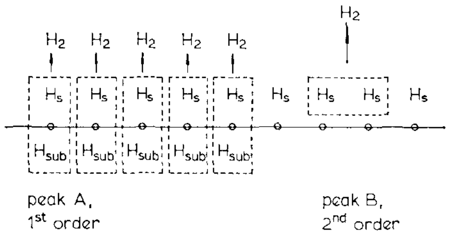

FIG. 5. Schematic representation of first- and second-order hydrogen desorption from palladium. Postulated mechanisms. (○) Surface site; (×) unique surface site for mechanism I; (H_s) surface hydrogen atom; (H_{sub}) subsurface hydrogen atom.

From (i), it follows that the occurrence of peak A is linked to desorption of hydrogen in excess of a coverage of 1. As argued by Lynch and Flanagan (7), hydrogen taken up above full coverage is in rapid equilibrium with absorbed hydrogen, and, therefore, it is reasonable to expect that it is atomic. How can this be reconciled with a first-order desorption which would point to a molecularly adsorbed form?

In order to answer this question, we suggest the desorption mechanism schematically represented in Fig. 5. Here, peak A represents hydrogen resulting from the recombination of a subsurface and a surface hydrogen atom. The interesting point is that such hydrogen is dissociatively adsorbed, but it desorbs from one site, and, hence, the desorption is first order in coverage. Peak B also represents desorption of atomically bound hydrogen, but, now, two *surface* hydrogens recombine, and, as two sites are involved here, desorption is second order in coverage.

The mechanism postulated above can still be subdivided into mechanism I, a porthole mechanism (see Fig. 5a), and mechanism II (see Fig. 5b), which we will call a breakthrough mechanism.

In mechanism I, all subsurface hydrogens desorb via *a relatively low number* of surface sites. Here, subsurface hydrogens diffuse through the palladium lattice to an octahedral interstice just below a surface octahedral-centered site, and hydrogen desorbs through recombination with an adsorbed hydrogen atom in the centered site. [In the (111) plane, a centered site is the hole formed by three closely packed surface atoms. Two types of centered sites are present: above tetrahedral interstices and above octahedral interstices.] If such a mechanism is operative, the total amount of surface hydrogen pulsed up to the kinkpoint should be equal to the amount desorbing as peak B, because hardly any surface hydrogens are consumed in the desorption of subsurface hydrogen.

In mechanism II, the breakthrough mechanism, subsurface hydrogen exclusively desorbs by recombination with surface hydrogens. Then, the amount desorbing as peak A is twice the amount of

TABLE 2

Volumes of Hydrogen per Gram of Catalyst Calculated from the Surface Areas of the TPD Peaks[a]

Expt No.	Volume calculated from pulse data in Table 1 [cm^3 H_2(NTP)/g of cat]				Volume of H_2 actually found in the TPD experiments [cm^3 H_2(NTP)/g of cat]	
	Mechanism I		Mechanism II			
	Peak A	Peak B	Peak A	Peak B	Peak A	Peak B[b]
1	0.65	1.80	1.29	1.16	0.59	1.86
2	0.00	0.49	0.00	0.49	0.01	0.52
3	0.00	0.98	0.00	0.98	0.01	1.04
4	0.49	1.90	0.97	1.41	0.81	1.58
5	0.19	1.55	0.39	1.36	0.52	1.23
6	0.72	1.33	1.44	0.61	1.37	0.68
7	0.51	1.30	1.03	0.79	1.14	0.67

[a] The volumes predicted from the pulse data in Table 1, according to mechanisms I and II, respectively, are compared with the volumes actually found in the TPD experiments. Results for sample 1.

[b] In calculating the area of peak B and the corresponding amount of hydrogen, the area of satellite peak B (see section *d* in Results) is included.

subsurface hydrogen, and the amount desorbing as peak B should be equal to the amount of hydrogen pulsed up to the kinkpoint minus half the amount desorbing as peak A.

In Table 2, we present the areas of peaks A and B, calculated as indicated above, starting from the pulse data in Table 1 for both mechanisms I and II.

The peak areas predicted from the pulse data according to mechanisms I and II are compared with the areas actually found in the TPD experiments following each pulse experiment. It is seen from Table 2 that, in four out of five cases in which adsorption in excess of one monolayer was involved, mechanism II showed good correlation between the pulse and TPD data, whereas mechanism I failed. For unknown reasons, the reverse is valid in experiment 1.

c. *The Enthalpy of Adsorption of "Type C" Hydrogen: Shape Analysis of Peak A*

For first-order desorption with freely occurring readsorption, the enthalpy of adsorption is calculated from Eq. (13) of the preceding paper (*12*). The total coverage, θ_i, was calculated from the ratio of hydrogen adsorbed in excess of a monolayer to the amount adsorbed in the monolayer. The coverage at $T = T_M$, θ_M, then, follows from Table 1 in Ref. (*12*). A^* in Eq. (13) in Ref. (*12*) is equal to exp $(\Delta S/R)$, where ΔS is the differential entropy of adsorption. By analogy with the entropy value reported by Lynch and Flanagan for weak "type C" adsorption on Pd, we took ΔS equal to $-83.6\ \mathrm{J \cdot mole^{-1} \cdot {}^\circ K^{-1}}$ (*7*).

The results are shown in column 4 in Table 3; the enthalpy of adsorption is about equal to that found by Lynch and Flanagan (*7*) for "type C" adsorption on palladium at $\theta = 0.3$, namely, 36.4 kJ/mole.

From a knowledge of ΔH and θ_i, the theoretical half-value peak width may be calculated from the theoretical peak shapes for first- and second-order desorption. First-order desorption leads to a better description than second order, though, in four out of five cases in Table 3, the experimental half-value peak width is somewhat smaller than the theoretical one (compare

TABLE 3

Enthalpy of Adsorption of "Type C" Hydrogen as Calculated from the Position of the Peak Maxima T_M of Type A Peaks[a]

Expt No. (1)[c]	T_M (2)	θ_i (3)	ΔH (kJ/mole) (4)	Half-value peak width (T/T_M units): Measured (5)	Theory: First order (6)	Theory: Second order (7)	Order n determined[b] (8)
1	283	0.28	29.0	0.116	0.123	0.196	1.12
4	297	0.21	33.0	0.136	0.148	0.208	1.26
5	293	0.17	32.6	0.172	0.152	0.192	1.26
6	297	0.52	36.0	0.136	0.174	0.228	1.00
7	291	0.44	34.7	0.124	0.164	0.224	0.97

[a] The half-value peak widths of A peaks are compared with the theoretical values for first- and second-order desorption. Sample 1.

[b] According to Kissinger (*21*).

[c] Column number.

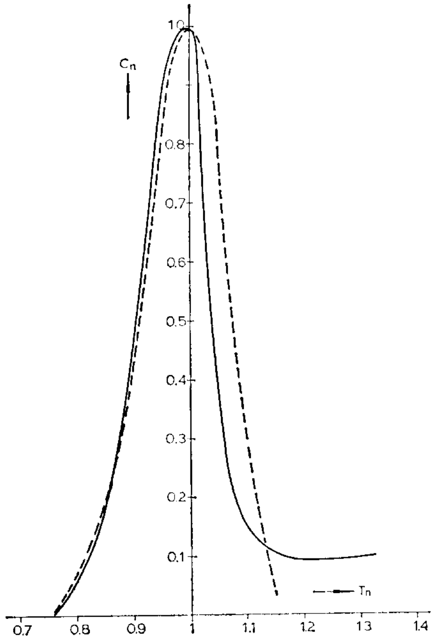

FIG. 6. Measured normalized peak shape of peak A (solid line), compared with the normalized theoretical peak shape for first-order desorption (dashed line). The meaning of the symbols C_n and T_n is given in Refs. (*11*) and (*12*).

columns 5, 6, and 7 in Table 3). The reason for this is unknown; theoretical peaks for first-order desorption without readsorption have half-value peak widths much smaller than the measured ones.

In Fig. 6, the experimental normalized peak shape corresponding to experiment 6 in Table 3 is compared with the theoretical normalized peak shape taken from Ref. (*11*). For the left-hand side of the peak, a perfect theoretical description is arrived at, whereas, for the right-hand side, the description is quantitatively unsatisfactory. The asymmetry in the experimental line was not found for all other A peaks measured; it appeared to be due to the fact that the top of the peak was rather flat, which made an exact determination of the top temperature rather difficult.

Another criterion for the order of desorption is formulated by Kissinger (*21*) for peak shapes found in differential thermal analysis (DTA). The starting points being the same as in the work of Cvetanović and Amenomiya (*11*) and in our work (*12*), Kissinger's criterion may be applied to peak-shape analysis in TPD as well. His method has an advantage in that the possible occurrence of fractional orders or a pseudo-zero order of desorption is included in the theory. The order of desorption, n, is given by (*21*):

$$n = 1.26 \times S^{\frac{1}{2}},$$

where S is the so-called shape index, defined as the ratio of the slopes of the tangents to the desorption curve at the inflection point.

Results are given in column 8 of Table 3; a mean value of $n = 1.08$ was calculated, and, hence, this method also points to a first order desorption process for all cases tabulated.

The order of desorption now being established, we can differentiate between the postulated porthole and breakthrough mechanisms. Interstitial diffusion of hydrogen through the bulk to the surface can be discarded as the rate-determining

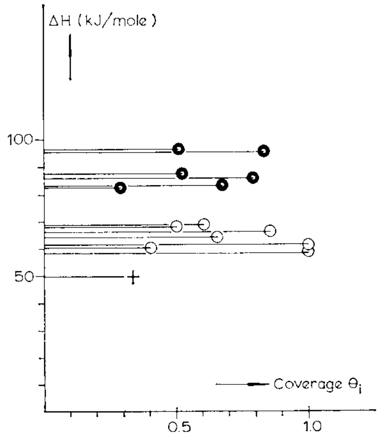

FIG. 7. Enthalpy of adsorption of normal dissociative hydrogen on palladium, as a function of coverage. Filled circles: sample 1, Pd on active carbon. Open circles: sample 2, Pd black with surface impurities. Cross: sample 3, highly contaminated Pd Mohr.

step, the activation energy for this process being lower than the activation energy measured [see Ref. (*18*)]. Porthole sites would immediately be refilled as soon as they are set free due to desorption, and a pseudo-zero-order behavior would result. As this is not observed, the porthole mechanism must be rejected.

d. The Enthalpy of Adsorption of Normal Dissociatively Chemisorbed Hydrogen: Shape Analysis of Peak B

As will be shown later, we are dealing here with second-order desorption, and, therefore, the enthalpy of adsorption must be calculated from Eq. (12) in Ref. (*12*). For all experiments with sample 1, the enthalpy of adsorption thus calculated is plotted in Fig. 7. In the calculation, it was assumed that the entropy loss during adsorption is equal to the entropy of gaseous hydrogen, the gas being adsorbed to immobility (*12*). The ΔH values in Fig. 7 are valid for $\theta = \theta_M$, as they are calculated from the top temperature, but, based on the fairly good correspondence between the measured and theoretical lineshapes (Fig. 8), it follows that ΔH is practically constant in the range of coverages from $\theta = \theta_i$ to $\theta = 0$, and this is the reason why, for each experiment, a line instead of a point was drawn in Fig. 7.

The small coverage sensitivity of ΔH is in accordance with the results of Conrad *et al.* (*6*) and Christmann *et al.* (*2*) for palladium and nickel, respectively. Furthermore ΔH is of the same magnitude as that reported for Pd(111), viz., 90 ± 5 kJ/mole.

For the highly contaminated samples 2 and 3, a ΔH value of 65 ± 10 kJ/mole was found (see Fig. 7). Obviously, large amounts of electropositive contaminations, like Zn, Pb, and Ca (detected in the ESCA analysis), and also carbon, produce a decrease in the enthalpy of adsorption of about 15%. On these highly contaminated samples, "type C" adsorption could not be detected.

Sample 1, intentionally contaminated with germanium (see Section *a* in Results), rapidly took up both hydrogen up to the kinkpoint and hydrogen in excess of a monolayer, and, in the succeeding TPD spectrum, both the A and B peaks are observed. Due to the presence of germanium, the Pd(3d $\frac{5}{2}$) line in the ESCA spectrum is shifted from 336.4 (Pd on carbon) to 335.4 eV. For the measurement, the carbon C(1s) line was taken as a reference. Hence, a chemical shift of 1 eV is found, indicating an increase in the electron density on the Pd sites.

Separate TPD experiments with the same samples revealed that, due to the presence of Ge, the top of the hydrogen B peak shifted from 407 to 383°K, which corresponds with a weakening of the Pd–H bondstrength of 2.7 kJ/mole. Obviously, electron donation of Ge to Pd weakens the hydrogen–palladium bond. A shift in the

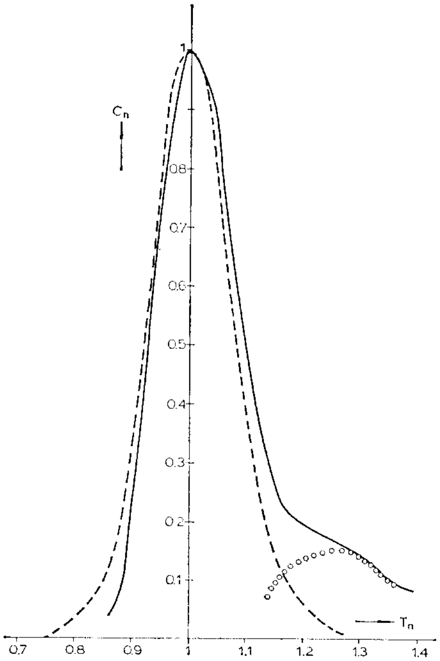

FIG. 8. Measured normalized shape of peak B (solid line), compared with the normalized theoretical peak shape for second-order desorption (dashed line). ΔH = 86 kJ/mole, θ_i = 0.25. (○) Satellite peak B; ΔH = 96 kJ/mole, θ_i = 0.03.

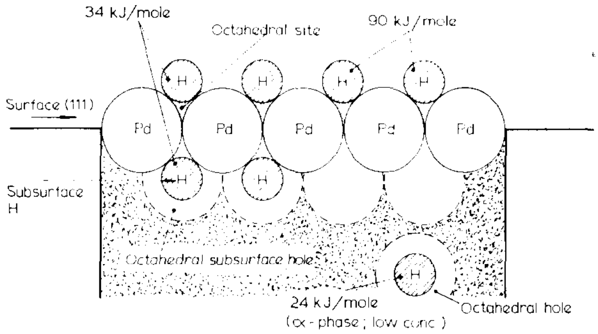

FIG. 9. Proposed mechanism for the desorption of bulk hydrogen from palladium, via the Pd(111) plane.

position of the A peak could not be detected within the accuracy of the experiment.

In Fig. 8, the experimental normalized peak B, found in experiment 2, Table 2, is compared with the normalized theoretical peak for second-order desorption, taken from Ref. (*12*). The theoretical curve is corrected for the temperature dependence of the adsorption entropy, as explained in Ref. (*12*). By subtracting the theoretical peak from the measured one, a satellite peak, B, can be isolated (see Fig. 8). Its area is about 10% of the total peak B area. The corresponding enthalpy of adsorption, calculated from the top temperature and the population, is calculated to be about 96 kJ/mole, whereas the same procedure gave a value of 93 kJ/mole for experiment 3 in Table 2. The nature of the binding mode represented by this satellite is in doubt. It may represent adsorption on the Pd(110) faces. This would be in accordance with the small percentage of these planes (*15*) and with the heat of adsorption reported by Conrad *et al.* (*6*) for Pd(110), viz., 102 kJ/mole.

DISCUSSION

The breakthrough mechanism introduced in this paper explains, in a natural way, how dissolved hydrogen can leave palladium via the surface, notwithstanding the fact that the chemisorbed layer is more strongly bound (90–100 kJ/mole) than the dissolved hydrogen (24 kJ/mole at low concentration in the α phase). The energy trap formed by the surface is easily surmounted by recombination of a subsurface and a surface hydrogen atom, by which the activation enthalpy of desorption is appreciably lowered (34 kJ/mole), as depicted in Fig. 9.

According to Lynch and Flanagan (*7*), hydrogen taken up in excess of a monolayer is adsorbed in interstitial *surface* sites, and this hydrogen is a precursor to interstitially *ab*sorbed hydrogen. Starting from this hypothesis, all our measurements can be explained in exactly the same way as done for hydrogen atoms adsorbed in excess in the octahedral subsurface holes; desorption of interstitial hydrogen atoms in the surface can also occur by recombination with the normal dissociatively chemisorbed hydrogen atoms. Again, a first-order desorption results, taking a coverage of 1 at the kinkpoint.

Within the framework of this study a firm decision between these two possibilities cannot be made.

There is even a third possibility, namely, that hydrogen adsorbed in excess of a monolayer is adsorbed in the molecular form. However, this view cannot be fully reconciled with our results, as it was found that desorption of hydrogen adsorbed in excess of the monolayer desorbs at the cost of the extent of the coverage of normally chemisorbed hydrogen (see Table 2). Moreover, a chemical bonding of hydrogen in the molecular form is difficult to imagine; in metal coordination chemistry, it is an unknown concept. Neither is a physical adsorption of hydrogen in the molecular form an attractive proposal, the enthalpy of adsorption of 34 kJ/mole, as found in this work for "type C" adsorption, being much too high for a physical interaction.

ACKNOWLEDGMENTS

The authors are grateful to Dr. G. Sawatsky, Physicochemical Department, State University of Groningen, The Netherlands, for carrying out, by electron spectroscopy, the surface analysis of the samples. Thanks are also due to Mr. J. C. Rasser, Department of Chemical Technology, Delft University of Technology, Delft, The Netherlands, for calculation of the theoretical lineshapes including the temperature dependence of the entropy.

REFERENCES

1. Sweet, F., and Rideal, E., *in* "Actes du Deuxième Congrès International de Catalyse, Paris, 1960," p. 175. Edition Technip, Paris, 1961.
2. Christmann, K., Schober, O., and Neumann, M., *J. Chem. Phys.* **60**, 4528 (1974).
3. Lapujoulade, J., and Neil, K. S., *J. Chem. Phys.* **70**, 798 (1973).
4. Bendorf, C., and Thieme, F., *Z. Phys. Chem. N.F.* **87**, 40 (1975).
5. Aldag, A. W., and Schmidt, L. D., *J. Catal.* **22**, 260 (1971).
6. Conrad, E., Ertl, G., and Latta, E. E., *Surface Sci.* **41**, 435 (1974).
7. Lynch, J. F., and Flanagan, T. B., *J. Phys. Chem.* **77**, 2628 (1973).
8. Dowden, D. A., *in* "Chemisorption" (W. E. Garner, Ed.). Butterworths, London, 1958.
9. Mignolet, J. C. P., *Bull. Soc. Chim.* **67**, 358 (1958).
10. Gundry, P. M., and Tompkins, F. C., *Trans. Faraday Soc.* **52**, 1609 (1956).
11. Cvetanović, R. J., and Amenomiya, Y., *in* "Advances in Catalysis" (D. D. Eley, H. Pines, and P. B. Weisz, Eds.), Vol. 17, p. 103. Academic Press, New York, 1967.
12. Konvalinka, J. A., Scholten, J. J. F., and Rasser, J. C., *J. Catal.* **48**, 377 (1977).
13. Scholten, J. J. F., and van Montfoort, A., *J. Catal.* **1**, 85 (1962).
14. U. S. Patent 3,962,139, June 8, 1976.
15. Sundquist, B. E., *Acta Met.* **12**, 67 (1964).
16. Aben, P. C., *J. Catal.* **10**, 224 (1968).
17. Sermon, P. A., *J. Catal.* **24**, 460 (1972); **24**, 467 (1972).
18. Fast, J. D., *in* "Gases in Metals," p. 126. N. V. Philips, Eindhoven, 1976.
19. Boudart, M., and Aldag, A. W., *J. Catal.* **18**, 146 (1970).
20. Mattson, J. S., and Mark, H. B., Jr., *in* "Activated Carbon," Chap. 3. Marcel Dekker, New York, 1971.
21. Kissinger, H. E., *Anal. Chem.* **29**, (11), 1703 (1957).